Korean J. Chem. Eng., 38(4), 807-815 (2021)
DOI: 10.1007/s11814-021-0742-3

pISSN: 0256-1115
eISSN: 1975-7220

Ammonia removal by adsorptive clinoptilolite ceramic membrane: Effect of dosage, isothermal behavior and regeneration process

Mohd Ridhwan Adam*, Mohd Hafiz Dzarfan Othman*,†, Siti Hamimah Sheikh Abdul Kadir, Muthia Elma***, Tonni Agustiono Kurniawan****, Ahmad Fauzi Ismail*, Mohd Hafiz Puteh*****, Azeman Mustafa*, Mukhlis A. Rahman*, Juhana Jaafar*, and Huda Abdullah******

*Advanced Membrane Technology Research Centre (AMTEC), School of Chemical and Energy Engineering, Universiti Teknologi Malaysia, 81310 UTM, Skudai, Johor, Malaysia
**Institute of Medical Molecular Biotechnology, Faculty of Medicine, Sungai Buloh Campus, Universiti Teknologi MARA (UiTM), Jalan Hospital, 47000, Sungai Buloh, Selangor, Malaysia
***Chemical Engineering Department, Engineering Faculty, Lambung Mangkurat University, 70714 Banjarbaru, South Kalimantan, Indonesia
****Key Laboratory of the Coastal and Wetland Ecosystems (Xiamen University), Ministry of Education, College of Ecology and the Environment, Xiamen University, Xiamen 361102 Fujian Province, P. R. China
*****School of Civil Engineering (FCE), Universiti Teknologi Malaysia, 81310 UTM, Skudai, Johor, Malaysia
******Department of Electrical, Electronic & Systems Engineering, Faculty of Engineering & Built Environment, The National University of Malaysia

(*Received 25 August 2020 • Revised 4 January 2021 • Accepted 5 January 2021*)

Abstract–This work investigates the effectiveness of ammoniacal nitrogen (NH_4^+-N) removal from contaminated water by adsorptive hollow fiber ceramic membrane (HFCM) derived from naturally made clinoptilolite. The technological value of this work is the simple mechanism of the adsorptive HFCM in removing gaseous ammonia in water by combining adsorption and separation. To test the technical feasibility of this proposed technology, clinoptilolite HFCM was fabricated via phase inversion-based extrusion/sintering technique and characterized by SEM and water permeation flux. The produced HFCM corresponds to the desired morphology of the asymmetric structure (dense and void formations) with outstanding adsorption performance of NH_4^+-N. The effects of the HFCM's operational parameters on its removal are examined in terms of membrane dosage and isothermal studies. The adsorption isotherm behavior exhibited that the adsorption process fitted the Freundlich isotherm model with outstanding removal performance even at trace concentration of ammonia. The low amount used by HFCM (4.75×10^{-4} m^2) resulted in over 96% ammonia removal, indicating a low cost of adsorption process. The regeneration of saturated HFCM suggests an outstanding recovery of the HFCM for its subsequent use for NH_4^+-N removal. This study also reveals the potential of adsorptive HFCM as a simple and cost-effective technology for ammonia removal from wastewater.

Keywords: Clinoptilolite, Hollow Fiber Ceramic Membrane (HFCM), Adsorptive Membrane, Ammoniacal-nitrogen Removal, Regeneration

INTRODUCTION

Rapid population growth is always accompanied by the increase in food demand. Agricultural technological intervention has been put to creating an upsurge in crop harvesting to fulfil these demands. Thus, the usage of fertilizers to boost crop production has become a widespread practice by agriculturally based industries in all parts of the world. Consequently, the wide usage of fertilizers that normally contain nitrogen-rich materials eventually contributes to the accumulation of ammoniacal nitrogen level in the environment [1]. Excess ammonia in water stream or reservoir may potentially lead to another hazardous problem. The eutrophication phenomenon driven by the undesirably high amount of ammonia will give rise to problems including algal bloom and toxification of fishes and aquatic lives as well as contamination of drinking water. Consequently, the problems are detrimental to human health upon the consumption of these ammonia-contaminated water and living stocks [2,3]. Therefore, the removal of ammonia and its constituent compounds from the water is crucial.

There are many conventional methods for ammonia removal from water. These include precipitation and flocculation, biological and chemical treatments, and adsorption and ion-exchange process [4-6]. Of all the methods, adsorption and ion-exchange processes possess the most promising and effective way of removing ammonia due to their simplicity, low cost, and high efficiency [7]. Additionally, new materials that are highly efficient for adsorption and ion exchange have gained tremendous attention and highlights for the past decades [8]. Among the studied materials, natural zeolite has gained much attention due to its large adsorption over surface area compared to other mineral materials.

†To whom correspondence should be addressed.
E-mail: hafiz@petroleum.utm.my

Clinoptilolite is the most abundant source of natural zeolite that is effective in removing ammonia from water since the 1970s [9]. Many studies have been reported on clinoptilolite utilization as an adsorbent for ammonia removal [10-13]. Nevertheless, these studies reported the adsorption process using clinoptilolite powder in suspension, which, to some extent, has many drawbacks. The inconvenient operation that needs a secondary filtration process, as well as high possibility of losing the adsorbent during the filtration, have become the major downsides of this powder suspension approach [14]. Therefore, a new approach that preserves the good adsorption properties of clinoptilolite accompanied by convenient practice and operation has become a new aim to improve the adsorption process.

The application of clinoptilolite in the form of adsorptive membrane for the elimination of ammonia is a novel and innovative approach. The utilization of the adsorbent in the form of a membrane was previously reported in the form of polymeric membranes [15-17]. Most of these polymeric hollow fibers are vulnerable to chemical and thermal stresses, resulting in morphological changes and membrane swelling. These fluctuations have weakening effects on the membrane execution [18]. Therefore, these polymeric membranes are restricted to only appliances with mild operational conditions, namely, low alkalinity and acidity as well as low temperature and pressure. As a solution to this problem, a new technique was established to construct ceramic hollow fiber membranes. Due to their superior thermal and chemical constancy, ceramic membranes are more outstanding compared to polymeric membranes in more extreme environments. The utilization of ceramic materials, specifically natural zeolite, in the development of adsorptive HFCM aiming for ammonia removal was reported in the literature [19,20]. Although some reports testified to the fabrication of the adsorptive clinoptilolite HFCM, there is a lack of reports on the adsorption mechanism and effect of membrane dosage [14,19]. This study investigated the adsorption mechanism of the membrane towards ammonia in synthetic wastewater. Furthermore, the regeneration of the saturated adsorptive membrane examined in this study adds to the novelty of this research. Instead of soaking and filtering the common adsorbent in the regenerant solution, the single backwashing approach with the regenerant was applied, which is simpler and novel compared to the common regeneration process. The outcomes give new perspective on the advancement of the adsorptive ceramic-based membrane in the wastewater treatment process.

EXPERIMENTAL

1. Fabrication and Characterization of Adsorptive Hollow Fiber Ceramic Membrane

Clinoptilolite powder with an average 70 μm size was procured from Shijiazhuang Mining Trade Co. Ltd., Ziaoning, China. Prior to the fabrication of the adsorptive membrane, the powder was ground and sieved into 36 μm and dried for 24 h to eliminate the moisture contained in the sample. Arlacel P135 (polyethyleneglycol 30-dipolyhydroxystearate, Uniqema), *N*-methyl-2-pyrrolidone, NMP (AR grade, QRëC), and polyethersulfone, PESf (Radal A300, Ameco Performance, USA) were used as dispersant, solvent, and polymer binder, respectively.

Adsorptive HFCM was prepared using phase inversion-based extrusion and sintering techniques [21-23]. First, 1 wt% Arlacel P135 (dispersant) was liquified in 49 wt% NMP (solvent) and vigorously stirred. Upon the formation of the homogeneous solution, 45 wt% of the pre-dried zeolite powder (ground and sieved into 36 μm) was gradually mixed into the slurry, and the formed suspension was projected to ball milling process using NQM-2 planetary ball mill. After 48 h of the milling process, 5 wt% of PESf was mixed into the dope and further milled for another 48 h. Upon completion of the milling process, the produced suspension was degassed (30 min) to remove trapped air to avoid defect formation in the membrane structure.

Before the extrusion process, the dope suspension was transferred into a syringe pump before being extruded through a tube-in-orifice spinneret using specified spinning parameters, namely, dope suspension extrusion rate of 10 mL/min, bore fluid extrusion of 15 mL/min, and air-gap distance of 5 cm. In this study, both the internal (bore fluid) and external coagulants used were tap water. After the extrusion process, the produced membrane precursors were further immersed in water coagulant to complete the phase inversion process. Subsequently, the membrane precursors were dried at room temperature. Lastly, the membrane precursors were sintered in air for 4 h at 1,050 °C [24]. In the sintering process, the heating and cooling rates used were 2 °C/min throughout the process. The fabrication of the adsorptive membrane in this study was previously described [25].

The morphology of the produced membranes was assessed at different magnification using scanning electron microscopy (SEM, Hitachi TM 3000, Japan). Prior to the analysis, each membrane was sputtered with platinum for 3 min under vacuum conditions. The morphology and cross-sectional anatomy of the membranes were analyzed. The membrane crystallography characteristics were also studied by X-ray diffraction (XRD) analysis. The XRD analysis was performed using XRD spectrometry (Bruker AXS D8, Germany), with a Cu Kα radiation (λ) of 1.5406 Å.

2. Membrane Adsorption Performance

2-1. Adsorption Analysis

The ammonia adsorption performance was evaluated using the crossflow water permeation system at 25 °C. The ammonia concentration in both feed (synthetic) and permeate solutions was determined using a UV-visible spectrophotometer (Hach Model DR 5000, Canada). This ammonia detection procedure was attained with the assistance of ammoniacal salicylate method that consisted of ammonium salicylate and ammonium cyanurate reagents as the color indicator for the ammonia concentration and measured at 644 nm. This method was formerly developed from the phenol or phenate method. In this process, the replacement of phenol by sodium salicylate thus removes the production of poisonous and highly volatile ortho-chlorophenol [26]. In this method, ammonia reacts with hypochlorite and produces monochloramine. The monochloramine subsequently reacts with salicylate and produces a blue-green compound known as 5-aminosalicylate. The color intensity of this compound is directly proportional to the concentration of the ammoniacal nitrogen in the sample [27]. The color intensity of this compound is measured by the absorbance and

interpreted into ammonia content. Ammonia removal is calculated by using the following equation:

$$R = \frac{C_f - C_p}{C_f} \times 100 \quad (1)$$

where C_f and C_p are the ammonia concentrations in the feed and permeate, respectively.

2-2. Adsorption Isotherm Experiments

The adsorption isotherm study of ammonia removal using the adsorptive HFCM was carried out by varying the initial ammonia feed concentration. The initial ammonia feed concentration ranged from 50 to 500 mg/L ammonia (0.1 L) at set conditions of 25 °C, pH 7, and 3 h of filtration process using one strand of adsorptive HFCM that weighed 0.1 g. All experiments were performed in triplicate (n=3). Results are presented as the mean and the standard deviations are indicated by the error bars.

2-3. Effect of HFCM amount Study

The effect of HFCM amount on ammonia adsorption was investigated by varying the number of HFCM from 1 to 5 strands. Each HFCM that was in contact with the feed ammonia solution had 1.58×10^{-4} m^2 of effective area and weighed 0.1 g. Table 1 represents the dosage of the membrane in terms of the number of membranes, effective area, and weight of the membranes. The experiment setup is shown in Fig. 1. The initial ammonia feed solution was fixed to 50 mg/L, and the pH, volume of the feed solution, and temperature were pH 7, 0.1 L, and 25 °C, respectively.

Table 1. Dosage of membrane for ammonia adsorption

Number of membranes	Effective area (m^2)	Weight (g)
1	1.58×10^{-4}	0.1
2	3.16×10^{-4}	0.2
3	4.75×10^{-4}	0.3
4	6.33×10^{-4}	0.4
5	7.91×10^{-4}	0.5

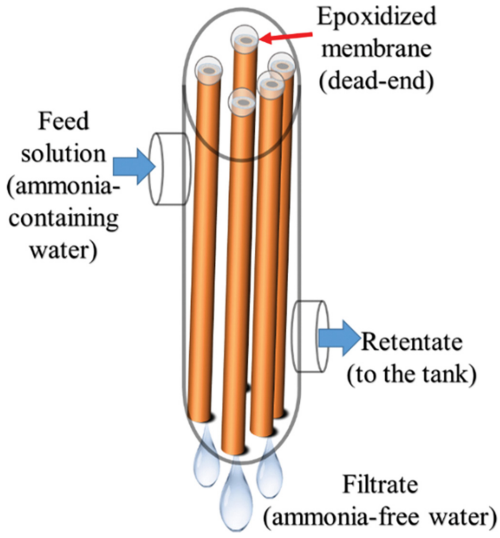

Fig. 1. Experimental setup of ammonia removal using the adsorptive HFCM.

The capacity of the HFCM adsorptivity was measured and determined using the following equation:

$$q_e = \frac{(C_i - C_e)V}{M} \quad (2)$$

where q_e is the adsorption capacity of the HFCM (mg/g), C_i is the initial ammonia feed concentration (mg/L), C_e is the ammonia concentration at equilibrium (mg/L), V is the volume of ammonia (L), and M is the weight of the HFCM (g).

3. Regeneration of the Adsorptive HFCM

The adsorptive HFCM was regenerated upon the decreasing of the ammonia uptake due to fully occupied active sites of the zeolite. Regeneration is the process whereby the adsorbed materials are taken out by a stripping solution, thus freeing the zeolite active sites and readying the HFCM for the next adsorption cycle. In this study, the used HFCM was backwashed with 5 g/L NaCl solution. The regenerated zeolite HFCM was cleaned and dried before the subsequent ammonia adsorption cycle. Fourier transform infrared spectroscopy analysis was carried out to determine the presence of functional groups in the sample before, during, and after ammonia adsorption process. This analysis confirmed the chemical changes due to the regeneration process. The analysis was performed by using IR Tracer-100 Shimadzu spectrophotometer at the resolution of 4,000 to 400 cm^{-1}.

RESULTS AND DISCUSSION

1. Morphological behavior of HFCM

The morphology of the HFCM sintered at 1,050 °C is shown in Fig. 2, where the SEM micrographs of the adsorptive HFCM were taken at various magnification. The fiber has an asymmetrical structure with both dense and void structures present. Several factors

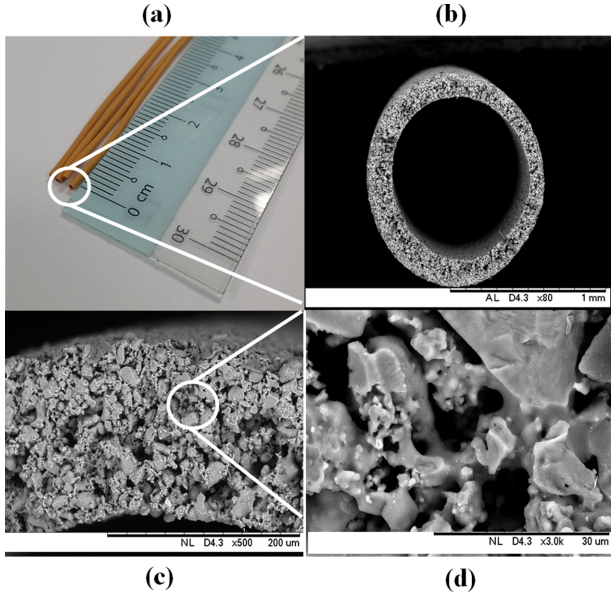

Fig. 2. The image of adsorptive HFCM (a) digital image; (b) overall cross-sectional SEM image; (c) zoom-in local cross-sectional SEM image; and (d) porous structure of SEM image at higher magnification.

could cause the formation of the voids. One of the factors is the demixing process during the phase-inversion technique. The interchange between solvent (NMP) with nonsolvent (water coagulant) during the phase-inversion process not only solidifies the membrane precursor from ceramic dope suspension but also forms the membrane's structural morphology. Theoretically, high miscibility of solvent-nonsolvent is favored in forming the finger-like structure, whereas low miscibility of solvent-nonsolvent is preferred in the sponge-like structure formation [28]. However, it is difficult to achieve a finger-like structure in ceramic membranes. One of the major causes is the irregular shape and size of the particle. Unlike its polymeric membrane counterpart, the ceramic suspension normally contains bigger particles (36 μm in this study), which eventually affects the formation of finger-like structure. This finger-like structure or voids could have have been attributed to the high flux of the membranes. However, this structure is considered as a defect because it sacrifices the mechanical strength of the ceramic membrane [29]. Additionally, it can be observed that the ceramic particles were integrated, thus attributed to the structure of the membrane. As discussed and reported in an earlier study, the HFCM structure is generally influenced by the sintering process of the membrane [30]. During the sintering process, the fine ceramic particle tends to be arranged uniformly with closely packed structure and thus reducing the pore or void formation between the ceramic particles. The high sintering temperature eventually promotes the grain growth process of the ceramic where the necking formation between the conjugated ceramic particles occurs. The interparticle spaces will allow good interaction between the ammonia and ceramic particles (adsorbent), thus enhancing the adsorption performance of ammonia by the membrane.

Fig. 3 shows the XRD patterns for natural zeolite and HFCM. The diffraction peaks at 2θ of 9.77°, 11.1°, 13.2°, 16.8°, 18.9°, 20.8°, 22.3°, 22.6°, 25.9°, 26.6°, 28.0°, 29.9°, 31.9°, 32.6°, 36.5°, and 50.1° were validated as natural zeolite. This was confirmed by the standard pattern of the clinoptilolite (01-079-1460 JCPDS card). The findings for this natural zeolite prove that the main phase was clinoptilolite. A similar finding was reported in a previous study [31]. In addition, apart from clinoptilolite, a small presence of cristobalite and quartz phases was detected in this sample. After the sintering process, the crystallinity of natural zeolite was changed significantly due to the heating process. The comparison between the two peaks (before and after sintering) showed a reduction in the peak's intensity for the heat-treated sample of the HFCM. This observation suggests that some of the crystal structure present in the non-sintered sample has become amorphous and can be proven by the reduction of some major peaks that corresponded to the clinoptilolite in the diffractogram. Meanwhile, the diffractogram of HFCM exhibited the presence of new major phases, namely, anorthoclase (01-077-8526 JCPDS card), cristobalite (01-077-8629 JCPDS card), and quartz (01-083-2187 JCPDS card). This observation indicates that these peaks belong to the crystal phase with a high melting point. Several studies have reported the same trend of findings in which different modifications have been done to the natural zeolite sample [32,33]. Note that the heating process (sintering) may reduce the natural zeolite's surface area by merging the natural zeolite particles via grain growth occurrence [34]. Additionally, the heating process has altered the phase behavior of the natural zeolite by profoundly enhancing the quartz and cristobalite (SiO_2 compounds), which may significantly occur due to the elimination of other elements or compounds during the sintering process. The copious presence of the SiO_2 compounds eventually affects the glassy state of the natural zeolite. Meanwhile, the better adsorption of ammonia by HFCM is mainly contributed by the existence of amorphous aluminosilicate compounds [34]. The superior adsorption of ammonia by this amorphous aluminosilicate compound is essentially contributed by the open structures that are responsible for the removal of ammonia from the water [35].

2. Adsorption of Ammonia onto HFCM

2-1. Adsorption Isotherms

The adsorption isotherms behavior of the ammonia onto the HFCM was studied using different adsorption isotherm models. The equilibrium adsorption capacity, Q_e of the HFCM onto the ammonia was studied and depicted in Fig. 4 as the function of different initial ammonia concentrations. The adsorption capacity

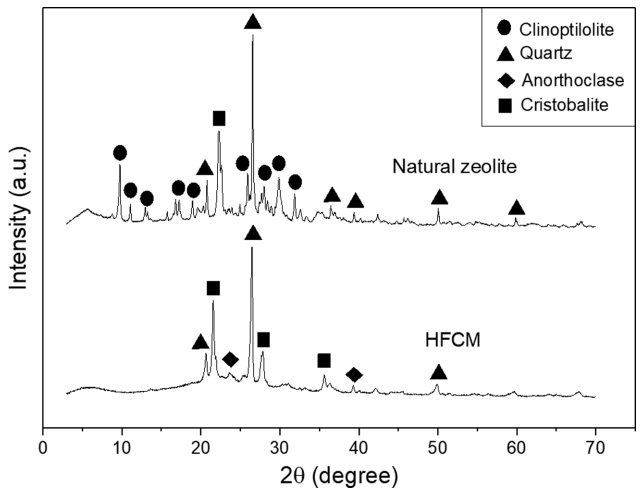

Fig. 3. The XRD patterns of the natural zeolite clinoptilolite and HFCM.

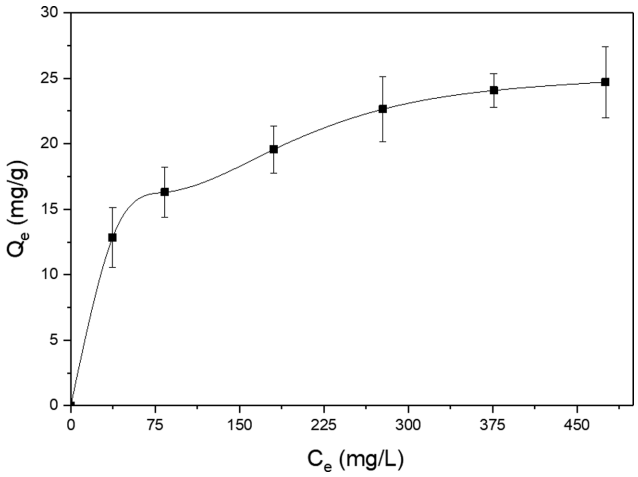

Fig. 4. The experimental adsorption isotherms of the ammonia onto the HFCM (n=3).

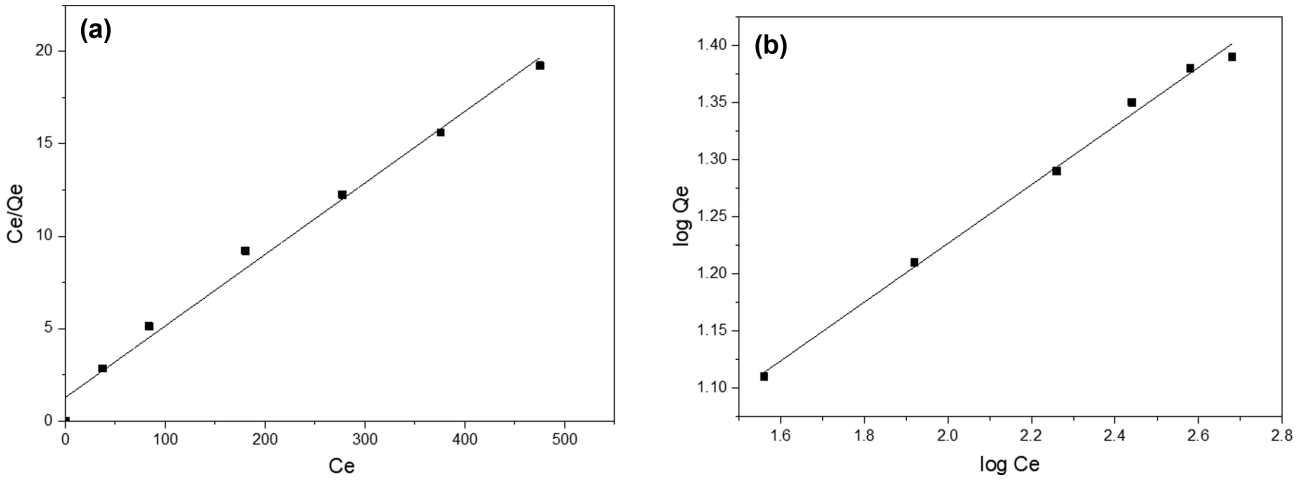

Fig. 5. The linear plots of (a) Langmuir and (b) Freundlich isotherm models.

increased along with the increment in the initial ammonia concentration from 50 to 500 mg/L. Further increases in the ammonia concentration showed no significant change in the adsorption capacity. Thus, this result suggests that the initial increment of ammonia concentration has intensified the driving force for mass transfer of the ammonia between the adsorbent phase of the HFCM and the aqueous medium. This phenomenon increases the adsorption capacity of the ammonia [36].

Additionally, the ammonia uptake process by the HFCM occurred rapidly and efficiently at low ammonia concentration. This result indicates that the HFCM is a suitable adsorbent even in low ammonia concentration environment such as in wastewater treatment facilities and eutrophic waters [37]. Moreover, the higher ammonia adsorption capacity by the HFCM is mainly attributable to the excellent ion exchange property possessed by the natural zeolite. The isomorphous substitution of the Al^{3+} to Si^{4+} in the lattice sheet of the zeolite eventually forms negatively charged adsorption sites. This active site then localizes to the surface of the particle and is likely to be neutralized by the counterions located at the surface such as Na^{+}, K^{+}, and Ca^{2+} that are easily substitutable with other ions in the contact solutions (NH_4^{+}) [38].

The adsorption isotherm behavior was further described by applying a number of equilibrium isotherm models. In this work, two main isotherm models were fitted to the experimental data: Langmuir and Freundlich. According to the Langmuir adsorption model, the adsorption of the adsorbate takes place at the homogeneous specific sites of the adsorbent. Furthermore, in most cases, monolayer adsorption is attained [39]. The linear correlation of the Langmuir model is as follows:

$$\frac{C_e}{q_e}=\frac{1}{Kq_{max}}+\frac{1}{q_{max}}C_e \tag{3}$$

where q_{max} is the maximum adsorption capacity (mg/g) and K is the Langmuir constant (L/mg).

On the other hand, the Freundlich isotherm model assumes heterogeneity of the surface, and the adsorption occurs at the sites with different adsorption energies. The linear expression of the model is as follows:

Table 2. Adsorption isotherm parameters for the adsorption of ammonia onto the HFCM

Isotherm model	Parameters		
Langmuir	q_{max} (mg/g)	K (L/mg)	R^2
	25.8	0.03	0.989
Freundlich	K_F (mg/g)/(mg/L)$^{1/n}$	n	R^2
	5.17	3.89	0.995

$$\log q_e=\log K_F+\frac{1}{n}\log C_e \tag{4}$$

where K_F is the Freundlich adsorbent capacity (mg/g)/(mg/L)$^{1/n}$ and n is the reciprocal of the reaction order.

The linear correlations of Langmuir and Freundlich isotherm models, as well as the adsorption isotherm parameters for the adsorption process of the ammonia onto the HFCM, are depicted in Fig. 5 and Table 2, respectively.

From the plots shown in Fig. 5 and parameters in Table 2, it can be concluded that the adsorption between ammonia and HFCM is best fitted to the Freundlich adsorption isotherm model with a coefficient of determination, R^2 value of 0.995, which is higher than that of Langmuir (0.989). The Freundlich isotherm constants K_f and n are determined from the intercept and slope of a plot of log Q_e versus log C_e in Fig. 5(b). The graph interpretation shows that the value of n is greater than unity (n>1), which indicates chemisorption interaction between the adsorbent and adsorbate [40]. Adsorption with an n value greater than unity is classified as L-type adsorption, reflecting chemisorption due to the high affinity between the adsorbate and adsorbent [41]. The adsorption capacity of the HFCM in this study is comparable to that of other adsorbents in the literature. This finding signifies that the HFCM is an economical and practical material for ammonia adsorption in water.

2-2. Effect of HFCM Dose

The effect of the ammonia adsorption by the adsorptive HFCM was further investigated by using different amounts of HFCM. Fig.

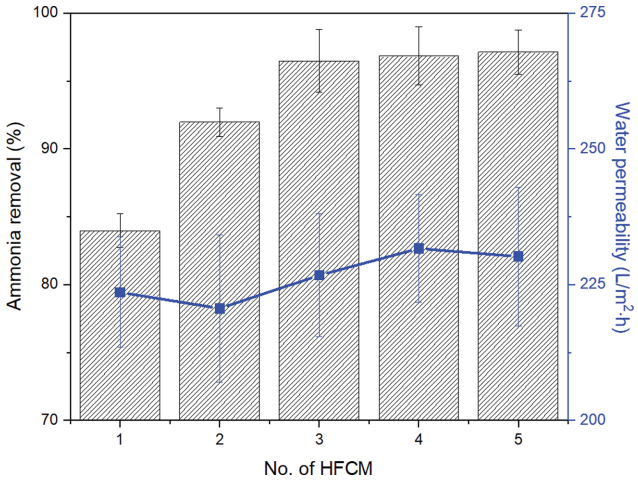

Fig. 6. The effect of HFCM amount on the water permeability and removal of ammonia (n=3).

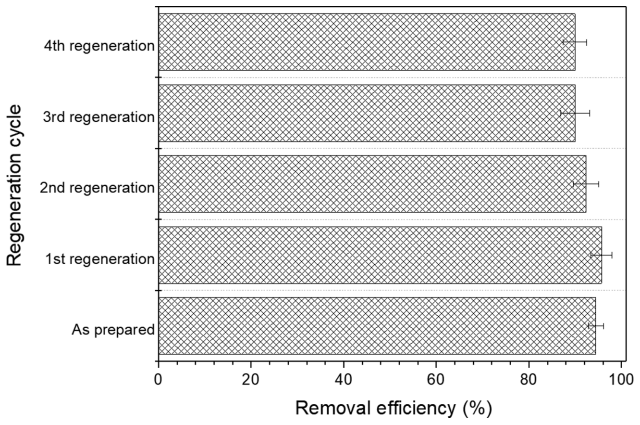

Fig. 7. The ammonia removal efficiency of HFCM at different regeneration cycle (n=3).

6 illustrates the removal efficiency of HFCM towards ammonia at different adsorbent dosages. Ammonia removal greatly increased to 96% when the HFCM amount was increased from one to three. This result could be attributed to the increment in the active sites available offered by the HFCMs, hence promoting more ammonia adsorption [42]. On the other hand, water permeability insignificantly increased upon the increment in the HFCM amount. Besides providing the available active sites for ammonia removal, the high amount of HFCM did not affect water permeability of the membrane. The fluctuating value of the water permeate from the HFCM was due to the same physicochemical behavior possessed by the HFCM sintered at the same temperature. The ammonia adsorption was significant when the number of HFCM increased from 1 to 3 strands. However, when the number was increased to 5 strands, the adsorption increment was slightly noticed. Although more ammonia was expected to be removed by high amounts of HFCM due to more active sites being offered, the slight increment in ammonia removal could be possibly due to insufficient residence time between the ammonia and the HFCM for the adsorption to take place due to the slightly higher water permeability of the HFCM. A similar trend was seen for the effect of flow rate in the breakthrough behavior study of adsorptive fixed-bed column system [43]. As the rate of the adsorbate leaving the adsorbent increases, the adsorption has a lower tendency to take place. This phenomenon can be explained by the fact that more physicochemical interactions happened between the HFCM adsorbent and the adsorbate. This result indicates that the flow rate of the adsorbate (ammonia) is the most critical factor in determining the efficacy of the HFCM adsorbent for ammonia adsorption [44]. Therefore, three was chosen as the best amount of HFCM for effective ammonia removal by considering the low cost due to low amount of HFCM and high ammonia removal efficiency up to 96% as it provides the highest removal efficiency in relation to the amount of HFCM used. This amount of HFCM was chosen and used for subsequent experiments.

3. Regeneration of HFCM

Regeneration is a common approach for the recovery of adsorptive materials. After much usage, the adsorbent undergoes a saturation process where the adsorbed species fully occupy the active sites of the adsorbent. This occurrence is known as the equilibrium point of the adsorbent [45]. The regeneration process of the saturated adsorbent is undertaken to recover the adsorbed species and free the active sites of the adsorbent for further adsorption process. In this study, 5 g/L NaCl was used as the regenerant solution for the recovery of the adsorbed ammonia from the HFCM membrane. Fig. 7 depicts the ammonia removal efficiency of the adsorptive HFCM over repeated regeneration cycles.

The relation shows that the removal efficiency of HFCM was stable with almost negligible loss of ammonia removal capacity throughout the sequential regeneration process. Additionally, the ammonia removal capacity of the HFCM slightly increased upon the first regeneration. This finding suggests that the regeneration of HFCM using the NaCl solution changed the zeolite of the HFCM into single ionic sodium form. This phenomenon subsequently increased the exchange property of the HFCM. Similar findings have been reported in a previous study in which the zeolite was studied in a column system [46]. After subsequent regeneration processes, the ammonia removal efficiency of the HFCM remained

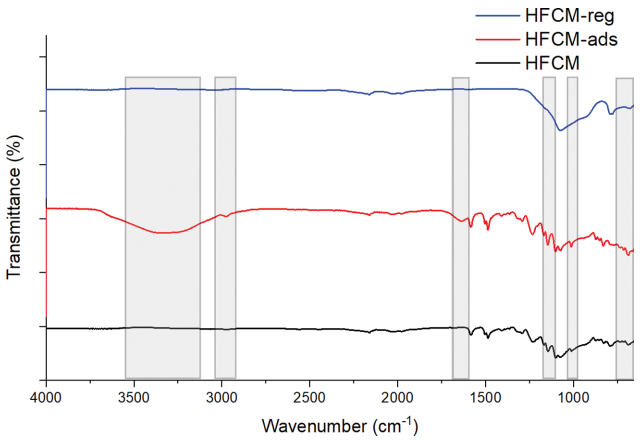

Fig. 8. The FTIR spectrum of adsorptive HFCM, ammonia-adsorbed HFCM and regenerated HFCM.

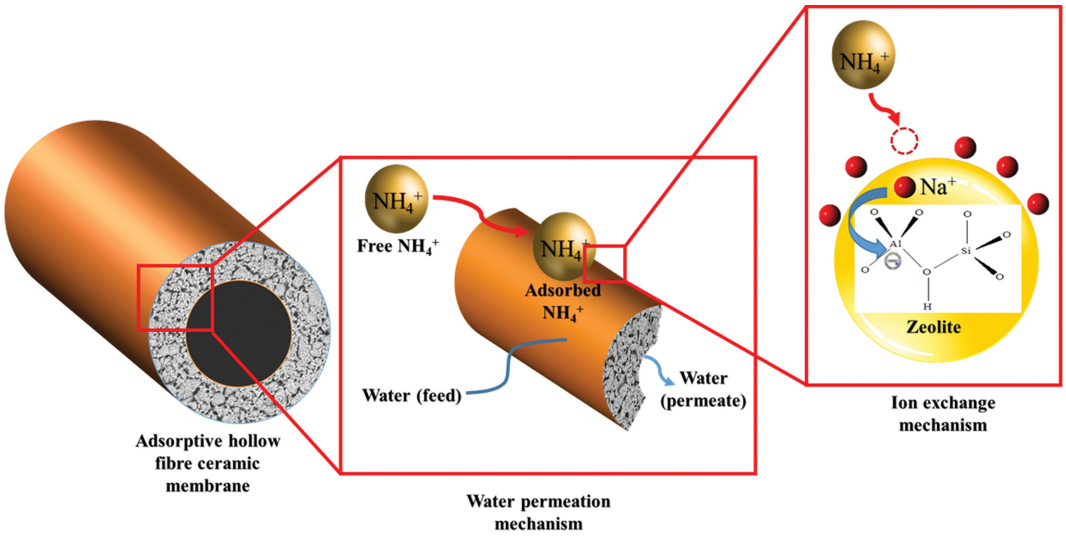

Fig. 9. The mechanism of ammonia adsorption by adsorptive HFCM.

constant with a slight decline. This result suggests that the regenerant solution activated the zeolite within the HFCM.

FTIR analysis further revealed the chemical interaction between the adsorptive membrane, ammonia, and the regenerant species. Fig. 8 depicts the FTIR spectra of adsorptive HFCM, ammonia-adsorbed HFCM, and regenerated HFCM. The spectrum shows the presence of the bands that are usually associated with aluminosilicate compound such as clinoptilolite zeolite. The band at around 1,100 cm^{-1} is assigned to the asymmetric stretching of SiO_4 tetrahedra. The shorter distance of the Si-O bond than Al-O bond and the presence of large amounts of other cations shifted the peaks to a higher wavenumber. The presence of a weaker shoulder at 1,000 cm^{-1} is assigned to vibration involving ≡Al-O created by the cation vacancies. The absorption peaks at 750-700 cm^{-1} correspond to the symmetric stretching vibration of SiO_4 groups. The stretching vibration of SiO_4 is shifted towards lower frequency, indicating the presence of the internal Si-O···HO-Si bonds. A study reported the infrared absorption bands of zeolite that was similar to this study [47]. Upon the adsorption process between adsorptive HFCM with ammonia solution, the presence of major bands was significantly observed. The bands usually associated with water molecules at around 3,400 and 1,640 cm^{-1} are found in the ammonia-adsorbed HFCM. Furthermore, bands related to the presence of ammonia appeared at regions 3,450-2,950 and 1,700-1,300 cm^{-1}, indicating the N-H stretching and N-H bending bands, respectively. The most significant band of this adsorbate is seen at 3,375 cm^{-1} indicating the N-H stretching vibration in the range of the degenerate stretching N-H mode of ammonia, thus suggesting the weak bond of NH_3 molecules [48]. Upon the regeneration process in the presence of NaCl, the major bands of ammonia disappeared. The disappearance of the bands representing ammonia was pronounced at the spectrum of regenerated HFCM, indicating that the adsorbed ammonia was desorbed from the HFCM attributable to the presence of the regenerant solution. The bands representing aluminosilicate reappeared in the regenerated HFCM spectrum, indicating that the membrane had been regenerated and was ready for subsequent adsorption processes. Fig. 9 illustrates the ion-exchange mechanism of the zeolite. The regeneration process of the ammonia-adsorbed HFCM is represented by the reversibility of the mechanism, where the adsorbed ammonia is replaced by the Na^+ ions contributed by the regenerant solution.

Additionally, the pH of the regenerant solution played a significant role in influencing the efficiency of the regeneration process. In this study, the pH of the regenerant was adjusted to 11-12 by NaOH solution. This step is crucial as such pH could recover the regeneration efficiency and reduce the volume of the regenerant [9]. The presence of hydroxide ions at alkaline pH contributes to the elimination of the adsorbed ammonia on the HFCM based on the following expression:

$$NH_4\text{–HFCM}+Na^+ \rightarrow Na\text{–HFCM}+NH_4^+ \quad (5)$$

$$NH_4^+ + OH^- \Leftrightarrow NH_3 + H_2O \quad (6)$$

The discharging of the adsorbed ammonia by the sodium ions from the regenerant solution occurs during the regeneration process, causing the ammonia to become free ions. Then, these ions are neutralized by the hydroxyl ions upon the completion of the regeneration process.

It is evident that pH does not affect Henry's constant but correlates with the distribution of species between ionized and unionized forms, which influences the overall gas-liquid distribution of the compounds. In this regard, the concentration of ammonia in the solution depends on the K_a of NH_4^+ ions alone.

$$[NH_3] = \frac{[NH_3 + NH_4^+]}{1 + \frac{[H^+]}{K_a}} = \frac{[NH_3 + NH_4^+]}{1 + 10^{pK_a - pH}} \quad (7)$$

where $[NH_3]$ is the free-ammonia concentration, $[NH_3+NH_4^+]$ is the total ammonia concentration, $[H^+]$ is the hydrogen ion concentration, and K_a is the acid ionization constant for ammonia. For this reason, pH is important for the removal of NH_4^+-N, as it helps to convert the solute ammonium ions into ammonia in the

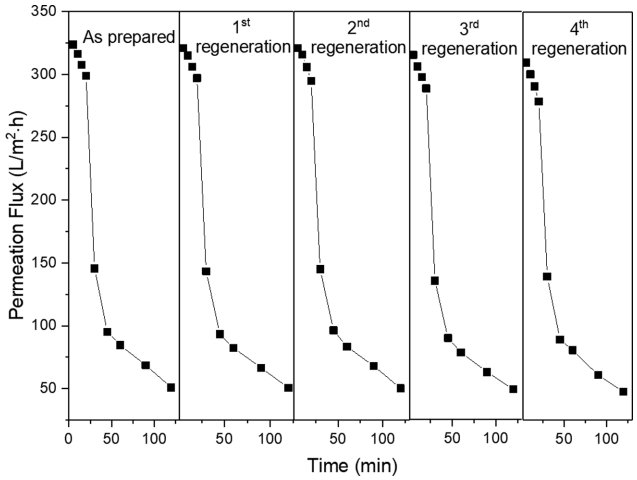

Fig. 10. The permeation flux of HFCM at a pressure of 1 bar in 4 regeneration cycles as compared to the prepared (first attempt) HFCM performance.

form of gas.

Apart from the uptake of the adsorbed ammonia from the saturated HFCM, the regeneration process also assists in the recovery of the HFCM water permeability. The permeation flux of the HFCM at different regeneration cycles is shown in Fig. 10.

The correlation shows that the regeneration successfully recovered the saturated HFCM and enhanced the permeability of the membrane. Apart from occupying the active sites of the HFCM, the adsorption of ammonia onto the membrane significantly exponentially reduced the permeability of the membrane. It is the properties of the ceramic materials that prolonged immersion and contact with water eventually cause the ceramic to swell [49]. This swelling phenomenon enhances the space between the mineral layers and adsorbs more water molecules between the layers [50]. The swollen membrane eventually deteriorates the water permeability of the membrane. The regeneration process of the saturated HFCM at high pH condition not only uptakes the adsorbed ammonia but also eliminates the adsorbed water molecules on the membrane through osmosis due to the concentration gradient. Therefore, the saturated HFCM is de-swelled during the regeneration process and subsequently increases the permeability of water in the next cycle of ammonia adsorption performance test. Fig. 11 illustrates the swollen and ammonia-adsorbed HFCM and the regenerated HFCM ceramic particles.

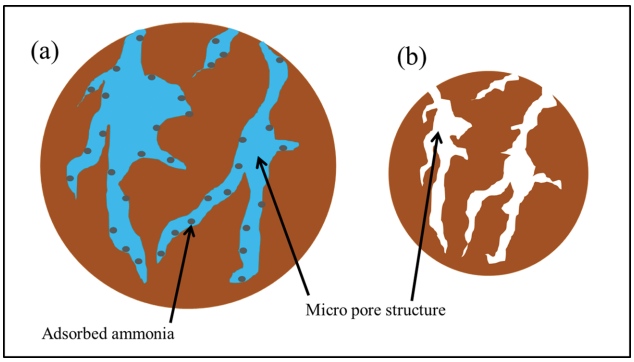

Fig. 11. The illustration of ceramic particles of (a) swollen ammonia adsorbed HFCM and (b) regenerated HFCM.

Unlike the conventional powder suspension adsorption process approach, the compact ceramic adsorptive membrane offers a hybrid process of separation and adsorption counterparts. The regeneration process can be easily performed as it is capable of reducing the loss of adsorbent due to the filtration process after the regeneration reaction [51,52]. Additionally, the simple and straightforward regeneration process will save time and cost as it is done simultaneously. Thus, this approach can be impactful for adsorption studies and the industrial players related to this research area.

CONCLUSION

A simple and reproducible attempt in ammonia removal was successfully performed in this study. Adsorptive hollow fiber ceramic membrane was successfully fabricated using natural zeolite, and the adsorption and separation processes were merged in a single step. The fabricated adsorptive HFCM possessed outstanding ammonia removal capability up to 96% even at low ammonia concentration, which is attributable to the excellent ion-exchange property of the natural zeolite. Additionally, the isotherm behavior of the adsorption process was best fitted to the Langmuir adsorption isotherm model, thus suggesting a physical interaction between the ammonia and adsorptive HFCM. Additionally, the low amount of HFCM required for the excellent ammonia removal indicates good economical aspect. Moreover, the regeneration process of the saturated HFCM successfully recovered the membrane with no significant deterioration of the membrane's adsorption performance for subsequent ammonia adsorption processes. Moreover, the water permeability of the saturated HFCM was highly retained in subsequent regeneration processes. This innovative perspective of adsorption process has filled the gap of reducing the dependability on conventional powder suspension adsorption approach, which requires high cost and much time due to its inconvenient process. Additionally, apart from the ammonia removal application from water, this adsorptive membrane has great potential in a broad range of adsorptive membrane applications for the removal of heavy metals and dyes from water.

ACKNOWLEDGEMENTS

The authors would like to acknowledge the financial support from the Ministry of Education Malaysia under Fundamental Research Grant Scheme (Project Number: R.J130000.7809.5F161), Malaysia Research University Network (MRUN) Grant (Project number: R.J130000.7851.4L878) and the Higher Institution Centre of Excellence Scheme (Project Number: R.J090301.7809.4J430). The authors would also like to thank Universiti Teknologi Malaysia for the funding under the Transdisciplinary Research Grant (Project number: Q.J130000.3509.05G75), UTM High Impact Research (UTMHIR) Grant (Project number: Q.J130000.2409.08G34) and Professional Development Research University (PDRU) Grant (Project number: Q.J130000.21A2.05E04). The authors would also like to thank Research Management Centre, Universiti Teknologi

Malaysia for the technical support.

CONFLICTS OF INTEREST

There are no conflicts of interest to declare.

REFERENCES

1. A. G. Capodaglio, P. Hlavínek and M. Raboni, *Rev. Ambient. e Agua*, **10**, 481 (2015).
2. D. M. Anderson, P. M. Glibert and J. M. Burkholder, *Estuaries*, **25**, 704 (2002).
3. J. Heisler, P. M. Glibert, J. M. Burkholder, D. M. Anderson, W. Cochlan, W. C. Dennison, Q. Dortch, C. J. Gobler, C. A. Heil, E. Humphries, A. Lewitus, R. Magnien, H. G. Marshall, K. Sellner, D. A. Stockwell and D. K. Stoecker, *Harmful Algae*, **8**, 3 (2008).
4. P. Ilies and D. S. Mavinic, *Water Res.*, **35**, 2065 (2001).
5. X. Yang, T. Fraser, D. Myat, S. Smart, J. Zhang, J. Diniz da Costa, A. Liubinas and M. Duke, *Membranes*, **4**, 40 (2014).
6. T. Zhang, L. Ding and H. Ren, *J. Hazard. Mater.*, **166**, 911 (2009).
7. Z. Feng and T. Sun, *Chem. Eng. J.*, **281**, 295 (2015).
8. X.-w. Cheng, Y. Zhong, J. Wang, J. Guo, Q. Huang and Y.-C. Long, *Micropor. Mesopor. Mater.*, **83**, 233 (2005).
9. Q. Du, S. Liu, Z. Cao and Y. Wang, *Sep. Purif. Technol.*, **44**, 229 (2005).
10. A. Gunay, *J. Hazard. Mater.*, **148**, 708 (2007).
11. D. Karadag, Y. Koc, M. Turan and B. Armagan, *J. Hazard. Mater.*, **136**, 604 (2006).
12. M. Sprynskyy, M. Lebedynets, A. P. Terzyk, P. Kowalczyk, J. Namieśnik and B. Buszewski, *J Colloid Interface Sci.*, **284**, 408 (2005).
13. I. Tosun, *Int. J. Environ. Res. Public. Health*, **9**, 970 (2012).
14. M. R. Adam, N. M. Salleh, M. H. D. Othman, T. Matsuura, M. H., Ali, M. H. Puteh, A. F. Ismail, M. A. Rahman and J. Jaafar, *J. Environ. Manage.*, **224**, 252 (2018).
15. P. Ahmadiannamini, S. Eswaranandam, R. Wickramasinghe and X. Qian, *J. Membr. Sci.*, **526**, 147 (2017).
16. R. J. Gohari, W. J. Lau, T. Matsuura and A. F. Ismail, *Sep. Purif. Technol.*, **118**, 64 (2013).
17. X. Zhang, X. Fang, J. Li, S. Pan, X. Sun, J. Shen, W. Han, L. Wang and S. Zhao, *J. Colloid Interface Sci.*, **514**, 760 (2018).
18. A. M. Barbe, P. A. Hogan and R. A. Johnson, *J. Membr. Sci.*, **172**, 149 (2000).
19. M. R. Adam, T. Matsuura, M. H. D. Othman, M. H. Puteh, M. A. B. Pauzan, A. F. Ismail, A. Mustafa, M. A. Rahman, J. Jaafar and M. S. Abdullah, *Process Saf. Environ.*, **122**, 378 (2019).
20. M. R. Adam, M. H. D. Othman, S. H. S. A. Kadir, M. N. Sokri, Z. S. Tai, Y. Iwamoto, M. Tanemura and S. Honda, *Membranes*, **10**, 63 (2020).
21. M. H. A. Aziz, M. H. D. Othman, N. A. Hashim, M. R. Adam and A. Mustafa, *Appl. Clay Sci.*, **177**, 51 (2019).
22. S. M. Jamil, M. H. D. Othman, M. H. Mohamed, M. R, Adam, M. A. Rahman, J. Jaafar and A. F. Ismail, *Int. J. Hydrogen Energy*, **43**, 18509 (2018).
23. S. K. Hubadillah, M. H. D. Othman, M. A. Rahman, A. F. Ismail and J. Jaafar, *Arab. J. Chem.*, **13**, 2349 (2020).
24. M. R. Adam, N. M. Salleh, M. H. D. Othman, T. Matsuura, M. H. Ali, M. H. Puteh, A. F. Ismail, M. A. Rahman and J. Jaafar, *J. Environ. Manage.*, **224**, 252 (2018).
25. M. R. Adam, M. H. D. Othman and M. H. Puteh, *Adsorptive natural zeolite ceramic membrane for ammonia removal in wastewater*, U.T. Malaysia, Editor. 2019, Universiti Teknologi Malaysia: Malaysia (2019).
26. H. Verdouw, C. J. A. Van Echteld and E. M. J. Dekkers, *Water Res.*, **12**, 399 (1978).
27. L. Zhou and C. E. Boyd, *Aquaculture*, **450**, 187 (2016).
28. G. R. Guillen, Y. Pan, M. Li and E. M. V. Hoek, *Ind. Eng. Chem. Res.*, **50**, 3798 (2011).
29. J. Luyten, A. Buekenhoudt, W. Adriansens, J. Cooymans, H. Weyten, F. Servaes and R. Leysen, *Solid State Ion.*, **135**, 637 (2000).
30. M. R. Adam, M. H. D. Othman, S. K. Hubadillah, M. H. Puteh, Z. Harun and A. F. Ismail, *Int. J. Eng., Trans. B Appl.*, **31**, 1398 (2018).
31. M. Moradi, R. Karimzadeh and E. S. Moosavi, *Fuel*, **217**, 467 (2018).
32. M. Amereh, M. Haghighi and P. Estifaee, *Arab. J. Chem.*, **11**, 81 (2018).
33. Z. Jamalzadeh, M. Haghighi and N. Asgari, *Front. Environ. Sci. Eng.*, **7**, 365 (2013).
34. M. C. d. Silva, H. Lira, L. l. d. Lucena, C. d. Rosa, O. d. Freitas and L. D. Normanda, *Adv. Mater. Sci. Eng.*, **2015**, 7 (2015).
35. E. Opiso, T. Sato and T. Yoneda, *Int. J. Oil, Gas Coal Technol.*, **12**, 197 (2016).
36. Y. Angar, N. E. Djelali and S. Kebbouche-Gana, *Environ. Sci. Pollut. Res.*, **24**, 11078 (2017).
37. A. Alshameri, C. Yan, Y. Al-Ani, A. S. Dawood, A. Ibrahim, C. Zhou and H. Wang, *J. Taiwan Inst. Chem. Eng.*, **45**, 554 (2014).
38. V. K. Jha and S. Hayashi, *J. Hazard. Mater.*, **169**, 29 (2009).
39. M. Uğurlu and M. H. Karaoğlu, *Micropor. Mesopor. Mater.*, **139**, 173 (2011).
40. J. Q. Jiang, C. Cooper and S. Ouki, *Chemosphere*, **47**, 711 (2002).
41. M. R. Taha, K. Ahmad, A. A. Aziz and Z. Chik, *Geoenvironmental aspects of tropical residual soils*, in Tropical residual soils engineering, Taylor & Francis Group, London (2004).
42. K. Saltalı, A. Sarı and M. Aydın, *J. Hazard. Mater.*, **141**, 258 (2007).
43. A. Ramirez, S. Giraldo, J. García-Nunez, E. Flórez and N. Acelas, *J. Water Process. Eng.*, **26**, 131 (2018).
44. S. Babel and T. A. Kurniawan, *J. Hazard. Mater.*, **97**, 219 (2003).
45. R. Elmoubarki, F. Z. Mahjoubi, H. Tounsadi, J. Moustadraf, M. Abdennouri, A. Zouhri, A. El Albani and N. Barka, *Water Resour. Ind.*, **9**, 16 (2015).
46. T. C. Jorgensen and L. R. Weatherley, *Water Res.*, **37**, 1723 (2003).
47. K. B. Yrappa and K. B. V. Suresh, *Asian J. Chem.*, **19**, 4933 (2007).
48. H. Wu, W. Zhou, F. E. Pinkerton, M. S. Meyer, G. Srinivas, T. Yildirim, T. J. Udovic and J. J. Rush, *J. Mater. Chem.*, **20**, 6550 (2010).
49. M. A. Agha, R. E. Ferrell, G. F. Hart, M. S. A. E. Ghar and A. Abdel-Motelib, *Appl. Clay Sci.*, **131**, 74 (2016).
50. M. K. Uddin, *Chem. Eng. J.*, **308**, 438 (2017).
51. M. R. Adam, M. H. D. Othman, R. A. Samah, M. H. Puteh, A. F. Ismail, A. Mustafa, M. A. Rahman and J. Jaafar, *Sep. Purif. Technol.*, **213**, 114 (2019).
52. C. H. Lin, C. H. Gung, J. J. Sun and S. Y. Suen, *J. Membr. Sci.*, **471**, 285 (2014).